Original Article

# Prostate Cancer Detection with Multiparametric Magnetic Resonance Imaging: Prostate Imaging Reporting and Data System Version 1 versus Version 2

**Zhao-Yan Feng[1], Liang Wang[1], Xiang-De Min[1], Shao-Gang Wang[2], Guo-Ping Wang[3], Jie Cai[1]**

[1]Department of Radiology, Tongji Hospital, Tongji Medical College, Huazhong University of Science and Technology, Wuhan, Hubei 430030, China
[2]Department of Urology, Tongji Hospital, Tongji Medical College, Huazhong University of Science and Technology, Wuhan, Hubei 430030, China
[3]Department of Pathology, Tongji Hospital, Tongji Medical College, Huazhong University of Science and Technology, Wuhan, Hubei 430030, China

## Abstract

**Background:** Prostate Imaging Reporting and Data System (PI-RADS) is a globally acceptable standardization for multiparametric magnetic resonance imaging (mp-MRI) in prostate cancer (PCa) diagnosis. The American College of Radiology revised the PI-RADS to address the limitations of version 1 in December 2014. This study aimed to determine whether the PI-RADS version 2 (PI-RADS v2) scoring system improves the diagnostic accuracy of mp-MRI of the prostate compared with PI-RADS v1.

**Methods:** This retrospective study was approved by the institutional review board. A total of 401 consecutive patients, with clinically suspicious PCa undergoing 3.0 T mp-MRI (T2-weighted imaging + diffusion-weighted imaging + DCE) before transrectal ultrasound-guided biopsy between June 2013 and July 2015, were included in the study. All patients were scored using the 5-point PI-RADS scoring system based on either PI-RADS v1 or v2. Receiver operating characteristics were calculated for statistical analysis. Sensitivity, specificity, and diagnostic accuracy were compared using McNemar's test.

**Results:** PCa was present in 150 of 401 (37.41%) patients. When we pooled data from both peripheral zone (PZ) and transition zone (TZ), the areas under the curve were 0.889 for PI-RADS v1 and 0.942 for v2 ($P = 0.0001$). Maximal accuracy was achieved with a score threshold of 4. At this threshold, in the PZ, similar sensitivity, specificity, and accuracy were achieved with v1 and v2 (all $P > 0.05$). In the TZ, sensitivity was higher for v2 than for v1 (96.36% vs. 76.36%, $P = 0.003$), specificity was similar for v2 and v1 (90.24% vs. 84.15%, $P = 0.227$), and accuracy was higher for v2 than for v1 (92.70% vs. 81.02%, $P = 0.002$).

**Conclusions:** Both v1 and v2 showed good diagnostic performance for the detection of PCa. However, in the TZ, the performance was better with v2 than with v1.

**Key words:** Multiparametric Magnetic Resonance Imaging; Prostate; Prostate Imaging Reporting and Data System Version 1; Prostate Imaging Reporting and Data System Version 2

## Introduction

Prostate multiparametric magnetic resonance imaging (mp-MRI) combines morphologic T2-weighted imaging (T2-WI) with at least two functional techniques, which may include diffusion-weighted imaging (DWI) as a marker of cellular density, dynamic contrast-enhanced (DCE) to assess neoangiogenesis, and magnetic resonance spectroscopic imaging (MRSI) to assess tumor metabolism.[1] However, different diagnostic centers and different readers may lead to a wide range of interpretations of mp-MRI findings, which may result in poor clinical testing performance. In 2012, the European Society of Urogenital Radiology (ESUR) published a standardized reporting system for mp-MRI called the Prostate Imaging Reporting and Data System (PI-RADS).[1] In PI-RADS version 1 (PI-RADS v1), a 5-point scale is used to assess cancer presence on T2-W,

Access this article online

Quick Response Code:

Website: www.cmj.org

DOI: 10.4103/0366-6999.191771

**Address for correspondence:** Dr. Liang Wang, Department of Radiology, Tongji Hospital, Tongji Medical College, Huazhong University of Science and Technology, Wuhan, Hubei 430030, China
E-Mail: wang6@tjh.tjmu.edu.cn



**Received:** 04-05-2016 **Edited by:** Yi Cui
**How to cite this article:** Feng ZY, Wang L, Min XD, Wang SG, Wang GP, Cai J. Prostate Cancer Detection with Multiparametric Magnetic Resonance Imaging: Prostate Imaging Reporting and Data System Version 1 versus Version 2. Chin Med J 2016;129:2451-9.

DWI, DCE, and MRSI. However, clear instructions on how to integrate the overall PI-RADS score were lacking. Many studies have hypothesized that the T2-WI, DWI, and DCE protocols make identical contributions. Several authors have calculated a PI-RADS sum score (scale from 3 to 15) by summing the 3 single scores.[2-5]

To address the limitations of v1 and to achieve a globally acceptable standard, the new PI-RADS v2 classification was proposed jointly by ESUR and the American College of Radiology in December 2014.[6] Unlike PI-RADS v1, v2 regulates the classification of final PI-RADS scores. DWI is decisive for evaluating the peripheral zone (PZ) as is T2-WI for the transition zone (TZ). DCE results should be reported as positive when there is early focal enhancement and as negative when there is no early focal enhancement or diffuse enhancement rather than using the curve-type analysis described in PI-RADS v1. DCE plays a subordinate role for the PZ but is needed for the further classification of PI-RADS 3 lesions on DWI. The main difference between a finding with a score of 4 and that with a score of 5 on T2-W and DWI is a diameter <1.5 cm or ≥1.5 cm if there is no evidence of invasive behavior.[7-9] Since the second version of PI-RADS was introduced, many studies have demonstrated its clinical utility.[10,11] However, to date, few clinical trials have published data comparing PI-RADS v1 and v2. Therefore, the purpose of our study was to compare the diagnostic performance of v1 and v2 for the detection of prostate cancer (PCa).

## Methods

### Patients

This retrospective study was approved by the institutional review board, and informed consent was obtained from all patients. We searched our institutional databases to identify consecutive patients who underwent prostate mp-MRI, including all sequences of T2-WI, DWI, and DCE, and those who had a prostate biopsy between June 2013 and July 2015. Initially, 585 patients were identified. Patients were excluded from the study if (1) the patient underwent prior treatment, including hormonal, irradiation, cryotherapy, or surgical therapies ($n$ = 121); (2) previous biopsies were performed within 12 weeks before the MR examination data ($n$ = 35); (3) the clinical data, such as prostate-specific antigen (PSA) serum levels, were incomplete ($n$ = 15); or (4) the MR images were of poor quality due to the presence of hip implants or movement artifacts ($n$ = 13). After exclusions, a total of 401 patients were included in the study population.

### Magnetic resonance imaging technique

In our institution, prostate MRI was performed before a transrectal, ultrasound-guided (TRUS) biopsy. The MR images were acquired with a 3.0 T system (MAGNETOM Skyra, Siemens Medical Solutions, Erlangen, Germany) using an 18-element body coil above and a spine coil underneath the pelvis. All examinations included multiplanar T2-W images, axial T1-W images, and axial DW MR images of the prostate with $b$ values of 0, 50, 200, 400, 600, 800, 1000, and 1500 s/mm$^2$. Apparent diffusion coefficient maps were reconstructed for qualitative and quantitative assessments of DWI. DCE images were then obtained using a fast three-dimensional (3D) T1-weighted gradient-echo volumetric interpolated breath-hold examination (T1-VIBE) in the same plane as the T2-W sequence. DCE images were obtained before, during, and after a fast bolus injection of a paramagnetic gadolinium chelate. The contrast agent was administered using a power injector (Medtron, Saarbruecken, Germany) followed by a 20-ml saline flush injection at a flow rate of 2.5 ml/s. After precontrast dual-flip angle T1 mapping (flip angle = 2°, 15°), multiphase DCE images (35 phases) were obtained every 8 s for 4 min and 44 s without breath holding. Perfusion curves were generated with Tissue 4D commercial software (Siemens Medical Solutions, Erlangen, Germany), which was available on the Siemens Workstation. The technical parameters of the MRI sequences are shown in Table 1.

### Pathologic evaluation

After the MRI examination, all patients underwent a TRUS 12-core template biopsy with cognitive targeting. TRUS-guided prostate biopsy was performed in all the patients within 1–35 (median 10) days. The biopsy was performed by a single experienced urologist with 20 years of experience using an ultrasound system (Hawk 2102, BK Medical, Denmark) equipped with a 5.1 MHz endocavitary probe and a spring-loaded biopsy gun with an 18-gauge core biopsy needle. The prostate was divided into 12 regions (base, middle third, apex, and the most lateral regions of the base, middle third and apex, bilaterally). The biopsy operator also reviewed the MRI reports and attempted to specifically target the lesions using visual registration. Notably, in our institution, a Likert-type 5-point subjective scale system (1 = highly unlikely and 5 = highly likely) was used at the time of initial MRI reporting; each lesion suspicious for neoplasm was described according to its location, size, shape, and signal characteristics, and all prostate MRI reports were verified by a radiologist (Liang Wang) with 15 years of uroradiology experience. Cores were individually labeled according to their location with respect to the biopsy scheme. Histopathological biopsy assessments were performed by an experienced pathologist (Guo-Ping Wang, with more than 10 years of experience) who was blinded to the MRI results. Each sample was histologically analyzed as cancerous or noncancerous, and the histopathological analysis report included the positive core with the respective Gleason grade, presence of benign prostatic hyperplasia, benign prostate tissue, prostatitis, atypical small acinar proliferation, and high-grade prostatic intraepithelial neoplasia.

### Image analysis

In this study, two radiologists with 5 and 4 years of experience and a minimum of 1000 prostate MRI readings analyzed the imaging studies in consensus. The reviewers were aware that the patients had been referred for an MRI on the suspicion of PCa; however, the reviewers were blinded to the clinical

results and histopathologic findings. To report the location of each lesion, the prostate gland was divided into sixteen regions of interest on the MRI scans.[12] First, all lesions are rated on a scale from 1 to 5 in each of the three MRI sequences (T2-WI, DWI, and DCE) according to PI-RADS v1 [Table 2].[1] The analysis in the present study was conducted by the patient rather than by prostate sector, and the lesion with the highest sum PI-RADS score for each mp-MRI scan was identified. We then obtained the overall PI-RADS score (1–5) by classifying the sum score according to the algorithm proposed by Röthke *et al*.[13] [Table 3]. Next, the readers again scored the lesions according to PI-RADS v2 and generated a PI-RADS score (1–5)[6] [Tables 4 and 5]. Patients were classified as having either TZ or PZ cancer if more than 70% of the cancer volume was in a single zone.[14] Visual examples for PI-RADS v1 and v2 are provided in Figures 1 and 2. After all MRI readings and subsequent TRUS biopsies were completed, a comparison analysis was performed between the correlated foci on the MRI and the histologic findings.

## Statistical analysis

All analyses were patient-based. The Kolmogorov-Smirnov test and Levene's *F*-test were used to test the normality and equality of variances. The Mann–Whitney *U*-test was used to compare the differences in baseline characteristics between the malignant and nonmalignant groups. A receiver

**Table 1: MRI parameters**

| Sequence | Technique | Repetition time/echo time (ms) | Section thickness (mm) | Intersection gap | Field of view (mm) | Matrix | Parallel imaging factor | Flip angle | Time of acquisition |
|---|---|---|---|---|---|---|---|---|---|
| T2-WI | Axial, coronal, sagittal | 6500–6874/104 | 3 | 0 | 180×180 | 384×346, 384×346, 384×304 | 2 | 160 | 3:16, 2:56, 2:38 |
| T1-WI | Axial turbo spin echo | 807/13 | 5 | 0 | 300×356 | 320×240 | NA | 160 | 3:06 |
| DWI | Axial single-shot echo-planar | 4500/85 | 3 | 0 | 214×171 | 90×72 | 2 | 90 | 4:08 |
| DCE | Axial three-dimensional T1-weighted spoiled gradient echo | 5.08/1.77 | 3.5 | 0.7 | 260×260 | 192×154 | 2 | 15 | 4:44 |

T2-WI: T2-weighted imaging; T1-WI: T1-weighted imaging; DWI: Diffusion-weighted imaging; DCE: Dynamic contrast-enhanced; NA: Not applicable; MRI: Magnetic resonance imaging.

**Table 2: Single-modality scores according to the ESUR panel**

| |
|---|
| Score criteria |
| T2-WI for the PZ |
| Uniform high SI |
| Linear, wedge-shaped, or geographical areas of lower SI, usually not well demarcated |
| Intermediate appearances not in categories 1/2 or 4/5 |
| Discrete, homogeneous low signal focus/mass confined to the prostate |
| Discrete, homogeneous low signal intensity focus with extracapsular extension/invasive behavior or mass effect on the capsule (bulging) or broad (>1.5 cm) contact with the surface |
| T2-WI for the TZ |
| Heterogeneous TZ adenoma with well-defined margins: "organized chaos" |
| Areas of more homogeneous low SI, however, well marginated, originating from the TZ/BPH |
| Intermediate appearances not in categories 1/2 or 4/5 |
| Areas of more homogeneous low SI, ill-defined: "Erased charcoal sign" |
| Same as 4, but involving the anterior fibromuscular stroma or the anterior horn of the PZ, usually lenticular or waterdrop-shaped |
| DWI |
| No reduction in ADC compared with normal glandular tissue; no increase in SI on any high *b*-value image (≥*b*800) |
| Diffuse, hyper SI on ≥*b*800 image with low ADC; no focal features; however, linear, triangular, or geographical features are allowed |
| Intermediate appearances not in categories 1/2 or 4/5 |
| Focal area(s) of reduced ADC but isointense SI on high *b*-value images (≥*b*800) |
| Focal area/mass of hyper SI on the high *b*-value images (≥ *b*800) with reduced ADC |
| DCE-MRI |
| Type 1 enhancement curve |
| Type 2 enhancement curve |
| Type 3 enhancement curve |
| (+1) For focal enhancing lesion with curve Types 2–3 |
| (+1) For asymmetric lesion or lesion at an unusual place with curve Types 2–3 |

DCE: Dynamic contrast-enhanced; MRI: Magnetic resonance imaging; PZ: Peripheral zone; TZ: Transition zone; SI: Signal intensity; DWI: Diffusion-weighted imaging; ADC: Apparent diffusion coefficient; T2-WI: T2-weighted imaging; T1-WI: T1-weighted imaging; BPH: Benign prostatic hyperplasia; ESUR: European Society of Urogenital Radiology.

operating characteristic (ROC) analysis was performed to evaluate the area under the ROC curve (AUC) of the PI-RADS v1 and v2 scoring systems. The AUCs, along with 95% confidence intervals, were compared using *Z*-test. Differences in sensitivity, specificity, and accuracy between overall v1 and v2 scores were tested using McNemar's test. Two-sided $P < 0.05$ was considered statistically significant. The statistical calculations were performed using SPSS 19.0 (SPSS, Chicago, IL, USA) and MedCalc version 11.4.2.0 (MedCalc statistical software, Mariakerke, Belgium).

## Results

Patient characteristics are shown in Table 6. The mean age of our study population was 64.4 ± 9.0 (standard deviation) years (range, 34–88 years). A total of 150 patients were diagnosed with PCa, of whom 95 were PZ and 55 were TZ.

The mean prostate volumes were 52.26 ml in patients with PCa and 51.59 ml in patients without histologically verified PCa ($P = 0.715$). The median baseline PSA level was 43.81 ng/ml (range, 1.38–1762.96 ng/ml) for PCa, which was higher than for the nonmalignant group (median, 7.15 ng/ml; range, 0.20–171.6 ng/ml, $P < 0.05$).

### Prostate Imaging Reporting and Data System

The results of the ROC analysis for T2-WI, DWI, and DCE, which were evaluated according to the PI-RADS scoring system as well as the combination of all 3 sequences in a sum score, are shown in Table 7.

In terms of a single PI-RADS scores, in both PZ and TZ, the AUC was highest for DWI followed by T2-WI and then DCE, with an average AUC of 0.869 for DWI (v1 and v2 had AUCs of 0.860 and 0.877, respectively) compared with 0.842 for T2-WI and 0.791 for DCE. For the PZ, the DWI score provided the highest AUC value, followed by DCE and T2-WI. On average, the AUCs were 0.927 for DWI, 0.816 for DCE, and 0.779 for T2-WI. For the TZ, T2-WI showed a higher AUC than that of DCE and DWI, with an average AUC of 0.961 for T2-WI compared with 0.748 for DCE and 0.714 for DWI.

When we pooled the data from both PZ and TZ, the AUCs were 0.889 for PI-RADS v1 and 0.942 for v2 ($P = 0.0001$). For the PZ alone, the AUCs were 0.916 for v1 and 0.930 for

**Table 3: Overall PI-RADS v1 score definition**

| PI-RADS | Definition | Overall score with T2, DWI, and DCE |
|---|---|---|
| 1 | Most probably benign | 3, 4 |
| 2 | Probably benign | 5, 6 |
| 3 | Indeterminate | 7–9 |
| 4 | Probably malignant | 10–12 |
| 5 | Highly suspicious for malignancy | 13–15 |

T2-WI: T2-weighted imaging; DWI: Diffusion-weighted imaging; DCE: Dynamic contrast-enhanced; MRI: Magnetic resonance imaging; PI-RADS: Prostate Imaging Reporting and Data System.

**Table 4: The revised PI-RADS v2**

| Score | Criteria |
|---|---|
| T2-WI for PZ | |
| 1 | Uniform signal hyperintensity (normal) |
| 2 | Linear, wedge-shaped, or diffuse mild hypointensity, usually indistinct margin |
| 3 | Heterogeneous signal intensity or noncircumscribed, rounded, moderate hypointensity |
| 4 | Circumscribed, homogeneously moderate hypointense focus or mass confined to prostate and <1.5 cm in greatest dimension |
| 5 | Same as 4 but ≥1.5 cm in greatest dimension or definite extraprostatic extension or invasive behavior |
| T2-WI for TZ | |
| 1 | Homogeneously intermediate signal intensity (normal) |
| 2 | Circumscribed hypointense or heterogeneous encapsulated nodule(s) (BPH) |
| 3 | Heterogeneous signal intensity with obscured margins Includes others that do not qualify as 2, 4, or 5 |
| 4 | Lenticular or noncircumscribed, homogeneous, moderately hypointense and <1.5 cm in greatest dimension |
| 5 | Same as 4, but ≥1.5 cm in greatest dimension or definite extraprostatic extension or invasive behavior |
| DWI | |
| 1 | No abnormality on ADC and DWI with high *b*-value (≥1400) |
| 2 | Indistinct hypointense on ADC maps |
| 3 | Focal mildly or moderately hypointense on ADC maps and isointense or mildly hyperintense on high *b*-value DWI (≥1400) |
| 4 | Focal markedly hypointense on ADC maps and markedly hyperintense on DWI with high *b* values (≥1400) and <1.5 cm on axial images |
| 5 | Same as 4 but ≥1.5 cm in greatest dimension or definite extraprostatic extension and invasive behavior |
| DCE | |
| Negative | No early enhancement, diffuse enhancement not corresponding to a focal finding on T2-WI and/or DWI, or focal enhancement corresponding to a lesion showing features of BPH on T2-WI |
| Positive | Focal enhancement and enhancement earlier than or contemporaneously with that of adjacent normal prostatic tissues and findings corresponding with findings suspicious for cancer on T2-WI and/or DWI images |

DCE: Dynamic contrast-enhanced; MRI: Magnetic resonance imaging; PZ: Peripheral zone; TZ: Transition zone; SI: Signal intensity; DWI: Diffusion-weighted imaging; ADC: Apparent diffusion coefficient; T2-WI: T2-weighted imaging; T1-WI: T1-weighted imaging; BPH: Benign prostatic hyperplasia; PI-RADS: Prostate Imaging Reporting and Data System.

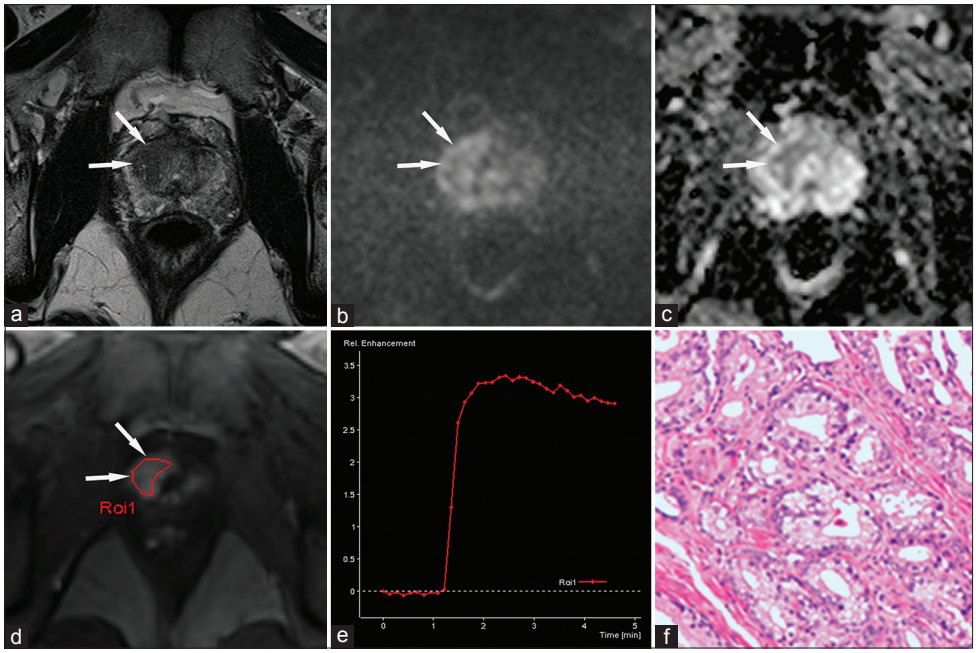


**Figure 1:** A 59-year-old male patient with a high prostate-specific antigen (23.938 ng/ml). (a) An axial T2-WI shows a hypointense area suspicious of cancer in the right transition zone at the mid-gland level (arrows); this area shows mild hyperintensity on the *b*-1500 s/mm$^2$ image of the DWI (b) and moderate hypointensity on the apparent diffusion coefficient map (c). On DCE (d), this area shows focal and early enhancement compared to the surrounding tissue. The signal intensity-time (SI-T) curve is Type II (e), and histology confirms prostate cancer (Gleason 3 + 4 = 7) (f). PI-RADS v1 scores: 4 points for T2-WI, 4 points for DWI, and 4 points for DCE, summed score = 12. This corresponds to a PI-RADS v1 score of 4. According to the PI-RADS v2 classification, the areas on T2-WI and DWI correspond to a score of 5 because they are larger than 1.5 cm and show a DCE that is "+" (early focal enhancement). Because the lesion is in the transition zone, the point value of T2-WI is significant for the PI-RADS v2 overall score of 5. PI-RADS: Prostate Imaging Reporting and Data System; DWI: Diffusion-weighted imaging; T2-WI: T2-weighted imaging; DCE: Dynamic contrast-enhanced.

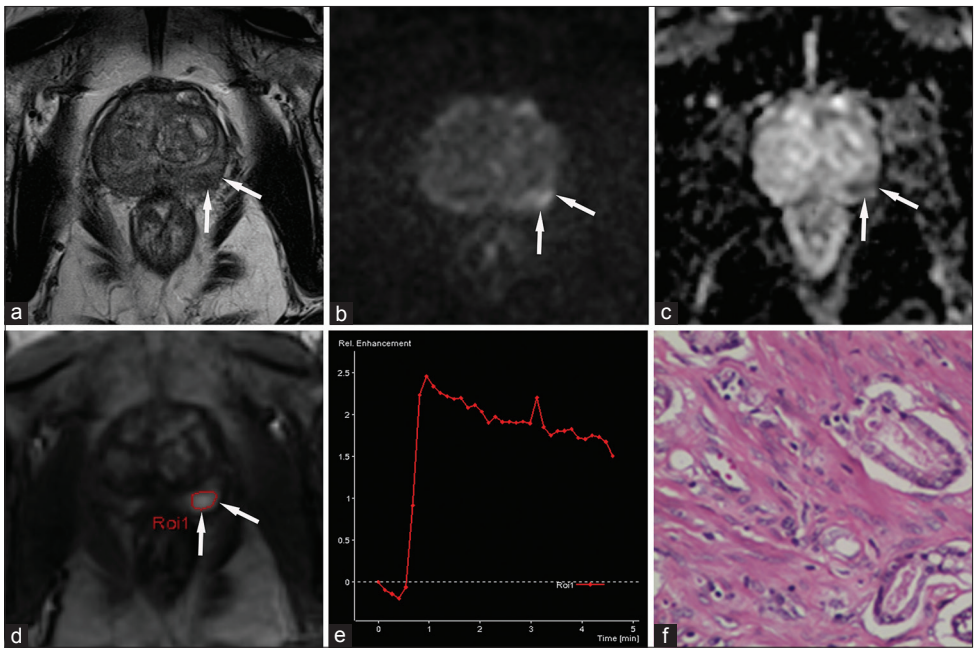


**Figure 2:** A 77-year-old male patient with a high prostate-specific antigen (8.995 ng/ml). (a) An axial T2-WI shows a heterogeneous signal in the peripheral zone. This area shows focal hyperintensity in the left peripheral zone (arrows) on the *b*-1500 s/mm$^2$ DWI (b) and hypointensity on the apparent diffusion coefficient map (c). On DCE (d), this area shows focal and early enhancement compared to the surrounding tissue. The SI-t curve is Type III (e), and histology confirms prostate cancer (Gleason 3 + 3 = 6) (f). PI-RADS v1 scores: 3 points for T2-WI, 5 points for DWI, and 5 points for DCE, summed score = 13. This corresponds to a PI-RADS score of 5. According to the PI-RADS v2 classification, the area on DWI corresponds to a score of 4 because it is smaller than 1.5 cm and shows a DCE that is "+" (early focal enhancement). Because the lesion is in the peripheral zone, the point value of DWI is significant for the PI-RADS v2 overall score of 4. PI-RADS: Prostate Imaging Reporting and Data System; DWI: Diffusion-weighted imaging; T2-WI: T2-weighted imaging; DCE: Dynamic contrast-enhanced.

v2 ($P = 0.3065$). For the TZ alone, the AUCs were 0.841 for v1 and 0.971 for v2 ($P < 0.001$).

ROC analysis was performed to determine the cutoff value that optimized the sensitivity, specificity, and accuracy for PCa detection [Table 8]. A cutoff value of 4 was used (scores of 4 and 5 were used as a positive mp-MRI). When we combined the two zones, PI-RADS v2 demonstrated significantly higher sensitivity (96% [144 of 150]) vs. 84.67% [127 of 150], $P < 0.001$), similar specificity (84.06% [211 of 251] vs. 81.27% [204 of 251], $P = 0.311$), and significantly higher accuracy (88.53% [355 of 401] vs. 82.54% [331 of 401], $P = 0.002$) than that of v1. We also evaluated the performance of the PI-RADS scoring system in TZ and PZ lesions separately. For the PZ, there were no differences in sensitivity, specificity, or accuracy using PI-RADS v1 compared with PI-RADS v2 (all $P > 0.05$). For the TZ, there was a significant improvement in sensitivity for PCa detection using PI-RADS v2 (96.36% [53 of 55]) compared with PI-RADS v1 (76.36% [42 of 55], $P = 0.003$); however, there was no difference in specificity using PI-RADS v2 (90.24% [74 of 82]) compared with PI-RADS v1 (84.15% [69 of 82], $P = 0.227$). Moreover, overall accuracy improved using PI-RADS v2 (92.70% [127 of 137]) compared with PI-RADS v1 (81.02% [111 of 137], $P = 0.002$).

**Table 5: Integration of MRI scores from T2-WI, DWI, and DCE from PZ and TZ recommended by PI-RADS v2**

| PZ | | | | TZ | | | |
|---|---|---|---|---|---|---|---|
| DWI | T2-WI | DCE | PI-RADS | T2-WI | DWI | DCE | PI-RADS |
| 1 | Any | Any | 1 | 1 | Any | Any | 1 |
| 2 | Any | Any | 2 | 2 | Any | Any | 2 |
| 3 | Any | Negative | 3 | 3 | ≤4 | Any | 3 |
| | | Positive | 4 | | 5 | Any | 4 |
| 4 | Any | Any | 4 | 4 | Any | Any | 4 |
| 5 | Any | Any | 5 | 5 | Any | Any | 5 |

Any: 1–5; T2-WI: T2-weighted imaging; DWI: Diffusion-weighted imaging; DCE: Dynamic contrast-enhanced; PZ: Peripheral zone; TZ: Transition zone; PI-RADS: Prostate Imaging Reporting and Data System; MRI: Magnetic resonance imaging.

## Discussion

There are some key differences between v1 and v2.[6-8,11,15,16]

**Table 6: Characteristics of patients enrolled in this study**

| Characteristic | All | PCa | Non-PCa |
|---|---|---|---|
| Number of patients | 401 | 150 | 251 |
| Age (years), mean (range) | 64.4 (34–88) | 66.7 (38–86) | 63.0 (34–88) |
| Prostate volume (ml), mean (range) | 51.84 (12.65–356.43) | 52.26 (13.36–356.43) | 51.59 (12.65–222.96) |
| PSA level (ng/ml), median (range) | 10.70 (0.20–1762.96) | 43.81 (1.38–1762.96) | 7.148 (0.20–171.6) |
| PI-RADS v1 on mp-MRI, *n* (%) | | | |
| 1 | 14 (4) | 0 (0) | 14 (6) |
| 2 | 64 (16) | 1 (1) | 63 (25) |
| 3 | 149 (37) | 22 (15) | 127 (51) |
| 4 | 109 (27) | 63 (42) | 46 (18) |
| 5 | 65 (16) | 64 (42) | 1 (0) |
| PI-RADS v2 on mp-MRI, *n* (%) | | | |
| 1 | 51 (13) | 1 (1) | 50 (20) |
| 2 | 89 (22) | 1 (1) | 88 (35) |
| 3 | 77 (19) | 4 (2) | 73 (29) |
| 4 | 54 (14) | 27 (18) | 27 (11) |
| 5 | 130 (32) | 117 (78) | 13 (5) |
| Prostate zone (*n*) | | | |
| PZ | | 95 | |
| TZ | | 55 | |
| Gleason score (*n*) | | | |
| ≤3+3 | | 17 | |
| 3+4 | | 29 | |
| 4+3 | | 50 | |
| ≥4+4 | | 54 | |
| Clinical stage (*n*) | | | |
| cT1 | | 3 | |
| cT2a | | 20 | |
| cT2b | | 16 | |
| cT2c | | 29 | |
| cT3a | | 12 | |
| cT3b | | 42 | |
| cT4 | | 28 | |

PSA: Prostate-specific antigen; PZ: Peripheral zone; TZ: Transition zone; PI-RADS: Prostate Imaging Reporting and Data System; PCa: Prostate cancer; mp-MRI: Multiparametric magnetic resonance imaging.

**Table 7: AUC values of single PI-RADS scores for T2-WI, DWI, and DCE and for summed PI-RADS score for cancer detection in PZ, TZ, and both PZ and TZ**

| Zone | T2-WI | | | DWI | | |
|---|---|---|---|---|---|---|
| | PI-RADS v1 | PI-RADS v2 | *P* | PI-RADS v1 | PI-RADS v2 | *P* |
| PZ and TZ | 0.834 (0.794, 0.869) | 0.849 (0.810, 0.883) | 0.0143 ($Z = 2.450$) | 0.860 (0.822, 0.892) | 0.877 (0.840, 0.907) | 0.0170 ($Z = 2.387$) |
| PZ | 0.777 (0.722, 0.826) | 0.780 (0.725, 0.828) | 0.7514 ($Z = 0.317$) | 0.919 (0.879, 0.949) | 0.934 (0.897, 0.961) | 0.0284 ($Z = 2.192$) |
| TZ | 0.957 (0.909, 0.984) | 0.965 (0.918, 0.989) | 0.2399 ($Z = 1.175$) | 0.705 (0.621, 0.780) | 0.723 (0.640, 0.796) | 0.2901 ($Z = 1.058$) |

| Zone | DCE | Overall | | |
|---|---|---|---|---|
| | PI-RADS v1 | PI-RADS v1 | PI-RADS v2 | *P* |
| PZ and TZ | 0.791 (0.747, 0.829) | 0.889 (0.854, 0.918) | 0.942 (0.915, 0.963) | 0.0001 ($Z = 3.980$) |
| PZ | 0.816 (0.763, 0.860) | 0.916 (0.876, 0.947) | 0.930 (0.893, 0.958) | 0.3065 ($Z = 1.023$) |
| TZ | 0.748 (0.667, 0.818) | 0.841 (0.769, 0.898) | 0.971 (0.928, 0.992) | <0.0001 ($Z = 4.411$) |

Data in parentheses are 95% *CI*s. AUC: Area under ROC curve; T2-WI: T2-weighted imaging; DWI: Diffusion-weighted imaging; DCE: Dynamic contrast-enhanced; PZ: Peripheral zone; TZ: Transition zone; PI-RADS: Prostate Imaging Reporting and Data System; ROC: Receiver operating characteristic; *CI*s: Confidence interval; MRI: Magnetic resonance imaging.

**Table 8: Diagnostic performance of PI-RADS v1 and v2 for PZ, TZ, and both PZ and TZ**

| Version | Both PZ and TZ | | | PZ | | | TZ | | |
|---|---|---|---|---|---|---|---|---|---|
| | Sensitivity | Specificity | Accuracy | Sensitivity | Specificity | Accuracy | Sensitivity | Specificity | Accuracy |
| PI-RADS v1 (%) | 84.67 | 81 | 82.54 | 89.47 | 79.88 | 83.33 | 76.36 | 84.15 | 81.02 |
| PI-RADS v2 (%) | 96 | 84 | 88.52 | 95.79 | 81.06 | 86.36 | 96.36 | 90.24 | 92.70 |
| *P* | <0.001 | 0.311 | 0.002 | 0.07 | 0.839 | 0.215 | 0.003 | 0.227 | 0.002 |

Cutoff values to differentiate between benign and malignant lesions were set to 4, with a score of 4 indicating clinically significant cancer being likely to be present. Diagnostic accuracy comparison between v1 and v2 using McNemar's test with $P<0.05$ considered statistically significant. PI-RADS: Prostate Imaging Reporting and Data System; PZ: Peripheral zone; TZ: Transition zone.

First, in v2, MRSI is no longer recommended for a PI-RADS assessment, with mp-MRI consisting only of T2-WI, DWI, and DCE. In contrast, v1 considers MRSI to be an optional technique. Second, in v2, the acquisition of high *b*-value images is recommended, utilizing a *b*-value of at least 1400 s/mm$^2$, whereas v1 recommends using ≥800 s/mm$^2$ as the high b-value series for interpretation. Third, subtle changes have been made to the 5-point scoring systems for T2-WI findings in the PZ and TZ and for the DWI findings. DCE has changed from a 5-point scale to being classified as either "positive" or "negative." In v1, it should be noted that the DCE score is very complex because it combines a 3-point score for three distinct curve types along with the focality and asymmetry of a finding to create a 5-point score. Most importantly, in v1, no recommendation is given on how to integrate the single scores for each sequence to calculate an overall score for a lesion.

Since the PI-RADS v1 scoring system was published in 2012, it has been evaluated in many studies.[17,18] In these previous studies, the sequence of T2-WI, DWI, and DCE was considered to have equal discriminatory power, and a sum score was used to integrate the individual scores for each sequence into an overall score for a lesion.[19-22] However, in v2, the concept of a "dominant sequence" was introduced. DWI is the key sequence for the PZ, and T2-WI predominates in the TZ. Details are provided on how to assign the final PI-RADS v2 score. In this study, we reported a single PI-RADS v1 score per patient on a 1-5 scale. Based on recommendations by Rothke *et al.*,[13] we added the individual scores to determine a total sum score and grouped it into five classes: PI-RADS scores of 3 and 4 were Class 1; 5 and 6 were Class 2; 7–9 were Class 3; 10–12 were Class 4; and 13–15 were Class 5.

In this study, we compared the diagnostic performance of v1 and v2. Summed PI-RADS v1 and v2 scores both showed good capability in cancer detection with a diagnostic accuracy of 0.80. The diagnostic accuracy increased from 0.82 to 0.88 with the use of v2 compared with v1 for all patients in our study cohort. The diagnostic accuracy values for the detection of TZ PCa were 0.81 for v1 and 0.92 for v2. The summed PI-RADS v2 outperformed v1 in the assessments of the TZ, and the two zones together and exhibited similar sensitivity, specificity, and accuracy in the assessment of the PZ. Our results indicate that diagnostic performance depends on cancer location. Our study is in accordance with other studies[5,23] that showed that DWI was the most effective method for identifying cancer in the PZ whereas T2-WI was more effective for tumors in the TZ. Literature comparing v2 and v1 is sparse. Polanec *et al*. reported that v2 appears to be the preferable method for evaluating the TZ whereas v1 performed better in the PZ.[24] Their findings are in accordance with our study and in that v2 shows improved performance in the TZ compared with v1. In contrast, our study indicates that v1 and v2 have a comparable diagnostic value in the PZ whereas their

findings showed that v1 performed better in the PZ and that the v1 approach should be used in PZ lesions. Another study by Kasel-Seibert compared v1 and v2 in ≥3 lesions and reported higher diagnostic accuracy using v2; however, the lesions were not analyzed separately based on the PZ and TZ.[25] These findings are of importance because v2 appears to improve TZ lesion classification, which is considered problematic to differentiate. Further study is required to determine v2 compared with v1 in classifying PZ lesions.

There are several limitations to the present study. The first is the use of a TRUS biopsy as the standard of reference due to the lack of whole-mount pathology slides after a radical prostatectomy. In China, PSA screening is not common, and the majority of patients are found to have high-grade PCa when diagnosed and are past the opportunity for a radical prostatectomy.[26] The majority of our study population with PCa had locally advanced disease, with Gleason score (GS) ≥4 + 3 comprising more than two-thirds of the cases and half of the patients with T3 + T4, which is likely to inflate the sensitivity because most institutions have predominantly GS 3 + 3 and 3 + 4 disease.[2,27] The second limitation is the spatial consistency between the MRI and the histopathological findings. A TRUS biopsy may be responsible for false-negative results if the tumor is small. In this study, we used MRI to direct the TRUS biopsy and focused primarily on the highest PI-RADS score. This patient-by-patient analysis, which did not include a per-region analysis, can partially obviate this problem.[28,29] Despite the limitations of our study, we believe that our methodical strategies provide sufficient validity for the principal results of our study.

In conclusion, PI-RADS v1 and v2 both performed well in tumor detection. PI-RADS v1 was somewhat less effective than v2 in the assessment of the TZ. The revised PI-RADS v2 should be studied further.


## Financial support and sponsorship

This study was supported by a grant of National Natural Science Foundation of China (No. 81171307).


## Conflicts of interest

There are no conflicts of interest.

## References


1. Barentsz JO, Richenberg J, Clements R, Choyke P, Verma S, Villeirs G, *et al.* ESUR prostate MR guidelines 2012. Eur Radiol 2012;22:746-57. doi: 10.1007/s00330-011-2377-y.
2. Rosenkrantz AB, Kim S, Lim RP, Hindman N, Deng FM, Babb JS, *et al.* Prostate cancer localization using multiparametric MR imaging: Comparison of prostate imaging reporting and data system (PI-RADS) and likert scales. Radiology 2013;269:482-92. doi: 10.1148/radiol.13122233.
3. Quentin M, Schimmöller L, Arsov C, Rabenalt R, Antoch G, Albers P, *et al.* 3-T in-bore MR-guided prostate biopsy based on a scoring system for target lesions characterization. Acta Radiol 2013;54:1224-9. doi: 10.1177/0284185113492972.
4. Rosenkrantz AB, Lim RP, Haghighi M, Somberg MB, Babb JS, Taneja SS. Comparison of interreader reproducibility of the prostate imaging reporting and data system and likert scales for evaluation of multiparametric prostate MRI. AJR Am J Roentgenol 2013;201:W612-8. doi: 10.2214/ajr.12.10173.
5. Baur AD, Maxeiner A, Franiel T, Kilic E, Huppertz A, Schwenke C, *et al.* Evaluation of the prostate imaging reporting and data system for the detection of prostate cancer by the results of targeted biopsy of the prostate. Invest Radiol 2014;49:411-20. doi: 10.1097/rli.0000000000000030.
6. Weinreb JC, Barentsz JO, Choyke PL, Cornud F, Haider MA, Macura KJ, *et al.* PI-RADS prostate imaging-Reporting and data system: 2015, version 2. Eur Urol 2016;69:16-40. doi: 10.1016/j.eururo.2015.08.052.
7. Muller BG, Shih JH, Sankineni S, Marko J, Rais-Bahrami S, George AK, *et al.* Prostate cancer: Interobserver agreement and accuracy with the revised prostate imaging reporting and data system at multiparametric MR imaging. Radiology 2015;277:741-50. doi: 10.1148/radiol.2015142818.
8. Franiel T, Asbach P, Teichgräber U, Hamm B, Foller S. Prostate imaging – An update. Rofo 2015;187:751-9. doi: 10.1055/s-0035-1553162.
9. Purysko AS, Rosenkrantz AB, Barentsz JO, Weinreb JC, Macura KJ. PI-RADS Version 2: A Pictorial Update. Radiographics 2016;36:1354-72. doi:10.1148/rg.2016150234.
10. Park SY, Jung DC, Oh YT, Cho NH, Choi YD, Rha KH, *et al.* Prostate Cancer: PI-RADS version 2 helps preoperatively predict clinically significant cancers. Radiology 2016;280:108-16. doi: 10.1148/radiol.16151133.
11. Vargas HA, Hötker AM, Goldman DA, Moskowitz CS, Gondo T, Matsumoto K, *et al.* Updated prostate imaging reporting and data system (PIRADS v2) recommendations for the detection of clinically significant prostate cancer using multiparametric MRI: Critical evaluation using whole-mount pathology as standard of reference. Eur Radiol 2016;26:1606-12. doi: 10.1007/s00330-015-4015-6.
12. Dickinson L, Ahmed HU, Allen C, Barentsz JO, Carey B, Futterer JJ, *et al.* Magnetic resonance imaging for the detection, localisation, and characterisation of prostate cancer: Recommendations from a European consensus meeting. Eur Urol 2011;59:477-94. doi: 10.1016/j.eururo.2010.12.009.
13. Röthke M, Blondin D, Schlemmer HP, Franiel T. PI-RADS classification: Structured reporting for MRI of the prostate. Rofo 2013;185:253-61. doi: 10.1055/s-0032-1330270.
14. McNeal JE. Regional morphology and pathology of the prostate. Am J Clin Pathol 1968;49:347-57.
15. Barentsz JO, Weinreb JC, Verma S, Thoeny HC, Tempany CM, Shtern F, *et al.* Synopsis of the PI-RADS v2 guidelines for multiparametric prostate magnetic resonance imaging and recommendations for use. Eur Urol 2016;69:41-9. doi: 10.1016/j.eururo.2015.08.038.
16. Barrett T, Turkbey B, Choyke PL. PI-RADS version 2: What you need to know. Clin Radiol 2015;70:1165-76. doi: 10.1016/j.crad.2015.06.093.
17. Hamoen EH, de Rooij M, Witjes JA, Barentsz JO, Rovers MM. Use of the prostate imaging reporting and data system (PI-RADS) for prostate cancer detection with multiparametric magnetic resonance imaging: A diagnostic meta-analysis. Eur Urol 2015;67:1112-21. doi: 10.1016/j.eururo.2014.10.033.
18. Wang X, Wang JY, Li CM, Zhang YQ, Wang JL, Wan B, *et al.* Evaluation of the prostate imaging reporting and data system for magnetic resonance imaging diagnosis of prostate cancer in patients with prostate-specific antigen <20 ng/ml. Chin Med J 2016;129:1432-8. doi: 10.4103/0366-6999.183419.
19. Renard-Penna R, Mozer P, Cornud F, Barry-Delongchamps N, Bruguière E, Portalez D, *et al.* Prostate imaging reporting and data system and likert scoring system: Multiparametric MR imaging validation study to screen patients for initial biopsy. Radiology 2015;275:458-68. doi: 10.1148/radiol.14140184.
20. Vaché T, Bratan F, Mège-Lechevallier F, Roche S, Rabilloud M, Rouvière O. Characterization of prostate lesions as benign or malignant at multiparametric MR imaging: Comparison of three scoring systems in patients treated with radical prostatectomy. Radiology 2014;272:446-55. doi: 10.1148/radiol.14131584.
21. Roethke MC, Kuru TH, Schultze S, Tichy D, Kopp-Schneider A, Fenchel M, *et al.* Evaluation of the ESUR PI-RADS scoring system for multiparametric MRI of the prostate with targeted MR/TRUS

fusion-guided biopsy at 3.0 Tesla. Eur Radiol 2014;24:344-52. doi: 10.1007/s00330-013-3017-5.
22. Schimmöller L, Quentin M, Arsov C, Hiester A, Kröpil P, Rabenalt R, *et al.* Predictive power of the ESUR scoring system for prostate cancer diagnosis verified with targeted MR-guided in-bore biopsy. Eur J Radiol 2014;83:2103-8. doi: 10.1016/j.ejrad.2014.08.006.
23. Ginsburg SB, Viswanath SE, Bloch BN, Rofsky NM, Genega EM, Lenkinski RE, *et al.* Novel PCA-VIP scheme for ranking MRI protocols and identifying computer-extracted MRI measurements associated with central gland and peripheral zone prostate tumors. J Magn Reson Imaging 2015;41:1383-93. doi: 10.1002/jmri.24676.
24. Polanec S, Helbich TH, Bickel H, Pinker-Domenig K, Georg D, Shariat SF, *et al.* Head-to-head comparison of PI-RADS v2 and PI-RADS v1. Eur J Radiol 2016;85:1125-31. doi: 10.1016/j.ejrad.2016.03.025.
25. Kasel-Seibert M, Lehmann T, Aschenbach R, Guettler FV, Abubrig M, Grimm MO, *et al.* Assessment of PI-RADS v2 for the Detection of Prostate Cancer. Eur J Radiol 2016;85:726-31. doi: 10.1016/j.ejrad.2016.01.011.
26. Zhang J, Xiu J, Dong Y, Wang M, Han X, Qin Y, *et al.* Magnetic resonance imaging-directed biopsy improves the prediction of prostate cancer aggressiveness compared with a 12-core transrectal ultrasound-guided prostate biopsy. Mol Med Rep 2014;9:1989-97. doi: 10.3892/mmr.2014.1994.
27. Kim JY, Kim SH, Kim YH, Lee HJ, Kim MJ, Choi MS. Low-risk prostate cancer: The accuracy of multiparametric MR imaging for detection. Radiology 2014;271:435-44. doi: 10.1148/radiol.13130801.
28. Grey AD, Chana MS, Popert R, Wolfe K, Liyanage SH, Acher PL. Diagnostic accuracy of magnetic resonance imaging (MRI) prostate imaging reporting and data system (PI-RADS) scoring in a transperineal prostate biopsy setting. BJU Int 2015;115:728-35. doi: 10.1111/bju.12862.
29. Wang R, Wang H, Zhao C, Hu J, Jiang Y, Tong Y, *et al.* Evaluation of multiparametric magnetic resonance imaging in detection and prediction of prostate cancer. PLoS One 2015;10:e0130207. doi: 10.1371/journal.pone.0130207.